International Journal of Nanomedicine

Dovepress
open access to scientific and medical research

Open Access Full Text Article

ORIGINAL RESEARCH

A personalized and long-acting local therapeutic platform combining photothermal therapy and chemotherapy for the treatment of multidrug-resistant colon tumor

This article was published in the following Dove Press journal:
International Journal of Nanomedicine

Beibei Wang[1]
Sunyi Wu[1]
Zhiqiang Lin[2]
Yajun Jiang[1]
Yan Chen[1]
Zhe-Sheng Chen[3]
Xiaoying Yang[1]
Wei Gao[1,4]

[1]Tianjin Key Laboratory on Technologies Enabling Development of Clinical Therapeutics and Diagnostics (Theranostics), School of Pharmacy, Tianjin Medical University, Tianjin 300070, China; [2]Institute of Systems Biomedicine, School of Basic Medical Sciences, Peking University Health Science Center, Beijing 100191, China; [3]College of Pharmacy and Health Sciences, St John's University, New York, NY 11439, USA; [4]College of Pharmacy, University of Michigan, Ann Arbor, MI 48109, USA

Correspondence: Xiaoying Yang; Wei Gao
Tianjin Key Laboratory on Technologies Enabling Development of Clinical Therapeutics and Diagnostics (Theranostics), School of Pharmacy, Tianjin Medical University, Tianjin 300070, China
Email yangxiaoying@tmu.edu.cn; gaowei841207@163.com

Background: Local photothermal therapy (PTT) provides an easily applicable, noninvasive adjunctive therapy for colorectal cancer (CRC), especially when multidrug resistance (MDR) occurs. However, using PTT alone does not result in complete tumor ablation in many cases, thus resulting in tumor recurrence and metastasis.

Materials and methods: In this study, we aim to develop a personalized local therapeutic platform combining PTT with long-acting chemotherapy for the treatment of MDR CRC. The platform consists of polyethylene glycol (PEG)-coated gold nanorods (PEG-GNRs) and D-alpha-tocopheryl PEG 1000 succinate (TPGS)-coated paclitaxel (PTX) nanocrystals (TPGS-PTX NC), followed by the incorporation into an in situ hydrogel (gel) system (GNRs-TPGS-PTX NC-gel) before injection. After administration, PEG-GNRs can exert quick and efficient local photothermal response under near-infrared laser irradiation to shrink tumor; TPGS-PTX NC then provides a long-acting chemotherapy due to the sustained release of PTX along with the P-glycoprotein inhibitor TPGS to reverse the drug resistance.

Results: The cytotoxicity studies showed that the IC_{50} of GNRs-TPGS-PTX NC-gel with laser irradiation decreased to ~178-folds compared with PTX alone in drug-resistant SW620 AD300 cells. In the in vivo efficacy test, after laser irradiation, the GNRs-TPGS-PTX NC-gel showed similar tumor volume inhibition compared with GNRs-gel at the beginning. However, after 14 days, the tumor volume of the mice treated with GNRs-gel quickly increased, while that of the mice treated with GNRs-TPGS-PTX NC-gel remained controllable due to the long-term chemotherapeutic effect of TPGS-PTX NC. The mice treated with GNRs-TPGS-PTX NC-gel also showed no weight loss and obvious organ damages and lesions during the treatment, indicating a low systemic side effect profile and a good biocompatibility.

Conclusion: Overall, the nano-complex may serve as a promising local therapeutic patch against MDR CRC with one-time dosing to achieve a long-term tumor control. The doses of PEG-GNRs and TPGS-PTX NC can be easily adjusted before use according to patient-specific characteristics potentially making it a personalized therapeutic platform.

Keywords: gold nanorods, paclitaxel nanocrystals, in situ hydrogel, tumor recurrence, TPGS

Introduction

Colorectal cancer (CRC), a cancer that starts in the colon or rectum, is one of the most prevalent and deadly tumor types among men and women worldwide. Especially in USA, CRC is the third most commonly diagnosed cancer according to the statistics in 2017.[1] Despite a decline in the incidence and mortality rate from the mid-1990s,

treating CRC still remains a considerable challenge.[2] Chemotherapy is an important strategy for treating CRC and delaying rapid recurrence of primary tumors.[3] However, in systemic chemotherapy, drug delivery to the tumor site is quite limited.[4] The low tumor drug distribution leads to off-target side effects and the development of multidrug resistance (MDR).[5] Long-term use of chemotherapeutics can upregulate the expression of ATP-binding cassette (ABC) transporters (mainly known as P-glycoprotein [P-gp]) on tumor cell membranes, which plays a crucial role in the mechanism of MDR.[6] Once the ABC transporters are upregulated, they efflux many types of drugs out of the tumor cells and protect them from cytotoxic harm.

Localized therapy is feasible for treating CRC, where anticancer agents can be administrated via either injection in the tumor site or implanting concurrently with tumor excision surgery.[7] Compared with systemic therapy, local therapy exerts antitumor efficacy directly to the site of tumor, thus providing better efficacy and minimizing off-target toxicity to healthy tissues.[8] Particularly, in the case of MDR tumor, local photothermal therapy (PTT) provides a promising adjunctive therapy by utilizing external near-infrared (NIR) light-induced hyperthermia to kill tumor cells through protein denaturation or rupture of the cellular membrane, while avoiding damages to the surrounding normal cells.[9,10] Gold nanorod (GNR) is one of the most commonly used agents in PTT due to its high efficient photothermal transition in the NIR region.[11] For example, Lee et al[12] investigated the feasibility of chemo-photothermal treatment on MDR tumors, and they demonstrated that PTT provided high therapeutic efficacy and low toxicity in the treatment of MDR tumors. However, using PTT alone does not result in complete tumor ablation in many cases due to the inhomogeneous heat distribution within tumor tissue; the residual tumor cells rapidly develop acquired resistance to thermal stress, resulting in tumor recurrence and metastasis.[13,14] To further improve the therapeutic index of tumors, PTT was combined with other modalities such as radiotherapy, chemotherapy, or photodynamic therapy.[15,16] For example, Conde et al[17] developed a novel local therapeutic gel patch, in combination with gene therapy, chemotherapy, and PTT, resulting in the tumor regression and the prevention of recurrence in colon cancer.

Drug nanocrystals (NCs) are newly emerged nanoplatforms that were formed by 100% hydrophobic drugs and stabilized by surfactants or polymeric steric stabilizers.[18] They not only can overcome solubility and bioavailability issues of poorly soluble drugs[19] but also can exhibit a long-term sustained drug release pattern in vivo.[20] Several NC formulations have already been used in clinical practice, such as Rapamune® (Pfizer, New York City, NY, USA), Tricor® (Abbott Lab., Chicago, IL, USA), and Emend® (Merck & Co., Kenilworth, NJ, USA).[21] Recently, Lin et al[22] developed a paclitaxel (PTX) NC-embedded gel system, which showed a good sustained release, high drug-loading profile, and long-time drug retention in the tumor site compared with the PTX gel and exhibited better antitumor efficacy on MCF-7 breast tumor-bearing mice.

Injectable hydrogel (gel) or in situ gel is one of the most promising biomaterials for developing local therapeutic systems.[23] This kind of system holds many advantages, such as good biocompatibility, easy for preparation and administration, biodegradability, and nontoxic degradation products.[24] Many types of in situ gels have been developed, which respond to different signals such as temperature, pH, and light.[23] Among them, poloxamers, namely Pluronic® (BASF, Ludwigshafen, Germany), are a class of commercially available materials, which are widely used in fabricating thermosensitive in situ gel. Poloxamers are ABA (PEO-PPO-PEO) triblock copolymers composed of hydrophilic polyoxyethylene (PEO) and hydrophobic polyoxypropylene (PPO, PEO–PPO–PEO). When the outside temperature exceeds a low critical solution temperature (LCST), it will undergo a phase transition from solution state to gel state.[25,26] By adjusting the formulations of the poloxamers and other excipients, the LCST can be tailored closely to body temperature, which allows the polymers to be injected into the body in a liquid state and followed by gelation at body temperature to form a cross-linked gel, thus achieving local retention and controlled release of the payloads.[23]

In this study, we aimed to develop a personalized and long-acting local therapeutic platform combining chemotherapy and PTT for the treatment of MDR CRC. PTX was used as the chemotherapeutic agent. It is a broad-spectrum anticancer drug with well-established antitumor efficacy, but shows very limited response in MDR tumor and induces multiple side effects including hair loss, bone marrow suppression, numbness, allergic reactions, muscle pains, diarrhea, heart problems, increased risk of infection, and lung inflammation.[27] The platform consists of dose-adjustable polyethylene glycol (PEG)-coated gold nanorods (PEG-GNRs) and D-alpha-tocopheryl PEG 1000 succinate (TPGS)-coated PTX NC (TPGS-PTX NC), followed by incorporation into a Pluronic P407 (F127)/Pluronic P188 (F68) in situ gel system before injection. After administration, the PEG-GNRs can exert quick and efficient local photothermal response within 5 minutes; TPGS-PTX NC later provides a long-term sustained release of PTX to reduce the risk of local recurrence along with the P-gp inhibitor

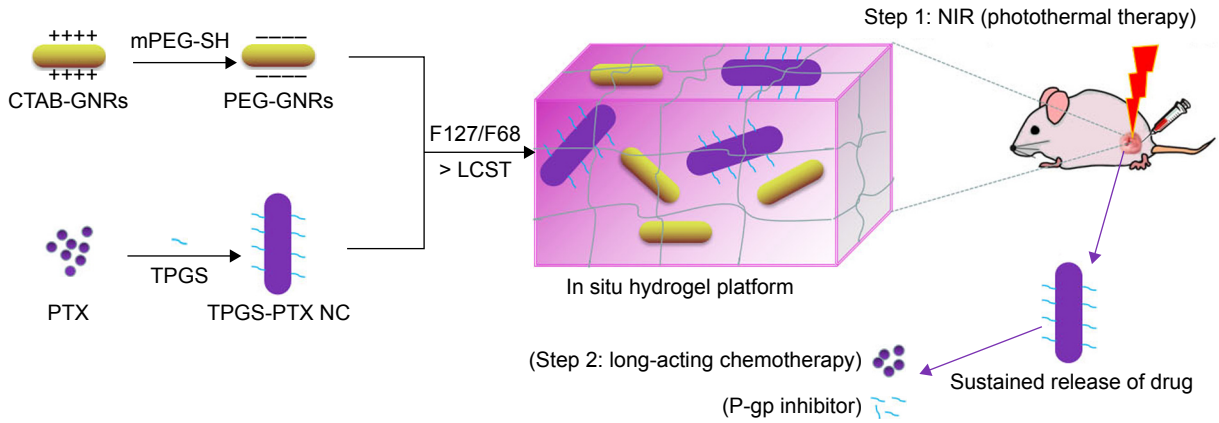

Figure 1 The illustration of the dose-adjustable in situ hydrogel platform containing PEG-GNRs and TPGS-PTX NC for the combination of PTT and long-acting chemotherapy.
Notes: CTAB-GNRs, CTAB-coated GNRs; PEG-GNRs, PEG-coated GNRs; TPGS-PTX NC, TPGS-coated PTX NC.
Abbreviations: CTAB, hexadecyl trimethyl ammonium bromide; GNRs, gold nanorods; LCST, low critical solution temperature; mPEG-SH, thiol-terminated methoxypoly-(ethylene glycol); NC, nanocrystal; NIR, near-infrared; PEG, polyethylene glycol; P-gp, P-glycoprotein; PTT, photothermal therapy; PTX, paclitaxel; TPGS, D-alpha-tocopheryl PEG 1000 succinate.

TPGS to reverse the drug resistance (Figure 1). The doses of PEG-GNRs and TPGS-PTX NC can be easily adjusted, at the time when it is mixed with gel, according to patient-specific factors. Characteristics of PEG-GNR, TPGS-PTX NC, and the gel system were studied in detail to confirm the quality of each unit of the platform. The in vitro release and erosion experiments proved that the gel system had a long-term sustained release of PTX. Cytotoxicity and animal experiments indicated that this system had good therapeutic effect on drug-resistant SW620 AD300.

Materials and methods

Materials

F127 and F68 were provided by BASF (Ludwigshafen, Germany). Thiol-terminated methoxypoly-(ethylene glycol) (mPEG-SH; molecular weight [MW] 5 kDa) was purchased from Suzhou Nord Derivatives Pharm-tech Co., Ltd. (Suzhou, China). Chloroform and sodium salicylate were purchased from Tianjin Chemical Reagent Supply and Marketing Company (Tianjin, China). Hexadecyl trimethyl ammonium bromide (CTAB) and TPGS were purchased from Sigma-Aldrich Co. (St Louis, MO, USA). Chloroauric acid ($HAuCl_4 \cdot 4H_2O$) was purchased from Fengchuan Chemical Reagent Co., Ltd (Tianjin, China). Sodium borohydride ($NaBH_4$), silver nitrate ($AgNO_3$), and ascorbic acid (AA) were purchased from Tianjin Heowns Chemistry Co., Ltd (Tianjin, China). PTX was purchased from Dalian Meilun Biology Technology Co., Ltd (Dalian, China). When used, PTX was dissolved in the mixture of Cremophor® EL (BASF) and dehydrated ethanol (50/50, v/v). DMEM, penicillin/streptomycin solution, trypsin–EDTA solution, and FBS were purchased from Biological Industries Israel Beit Haemek Ltd (Tianjin, China). MTT was purchased from Beijing Solarbio Science & Technology Co., Ltd (Tianjin, China). All other reagents are of analytical grade and were used without further purification. Purified water was produced by a Millipore water purification system.

Preparation of the GNRs-TPGS-PTX NC-gel system

Synthesis of GNRs

GNRs were synthesized by a seed-mediated growth method.[28] Briefly, $HAuCl_4$ aqueous solution (0.5 mM, 5 mL) was mixed with CTAB (0.2 M, 5 mL) and ice-cold $NaBH_4$ aqueous solution (10 mM, 600 µL) and stirred for 2 minutes to form a brown seed solution (solution A). Solution A was stored at 28°C for subsequent use. The growth solution (solution B) was prepared by mixing $AgNO_3$ solution (4 mM, 5 mL), CTAB (0.2 M, 100 mL), and $HAuCl_4$ (1 mM, 100 mL) and stirred for 6 minutes, followed by adding AA solution (78.8 mM, 1.45 mL) and stirred for another 4 minutes. Then, 420 µL of solution A was added into solution B and stirred at 500 rpm for 20 minutes. The mixture was continuously stirred for 4–6 hours allowing it to fully react and then centrifuged twice (13,000 rpm, 30 minutes) to remove the extra CTAB and obtain CTAB-coated GNRs (CTAB-GNRs).

Synthesis of PEG-GNRs

CTAB-GNRs were centrifuged at 13,000 rpm for 30 minutes and resuspended in an aqueous solution of SDS (0.08%). mPEG-SH solution was added into the GNR solution. The mixture was stirred overnight at room temperature, and then

it was centrifuged and re-dispersed in purified water twice to remove the excess CTAB and mPEG-SH. The excess mPEG-SH was quantified by the Ellman's assay to determine whether the reaction was complete.

Preparation of the TPGS-PTX NC

PTX and TPGS (or F127) with the weight ratio of 1:5 were first dissolved in chloroform. Then, the chloroform was volatilized under a steady stream of nitrogen gas. It underwent rotary evaporation to remove residual chloroform and obtain a dry film of PTX and TPGS (or F127). Certain amount of purified water was added to the dried film and incubated for 40 minutes, vortexed for 10 minutes, and sonicated for 15 minutes to obtain a uniformly transparent PTX NC suspension such as TPGS-PTX NC or F127-PTX NC.

Preparation of various gel systems

Blank gel was prepared by adding F127 and F68 into a certain amount of purified water to reach a final concentration of F127 at 22.5% and F68 at 2.5%. The mixture was stirred with the magnetic stirrer in a 4°C refrigerator until a clear solution was formed. TPGS-PTX NC-gel and GNRs-gel were prepared according to the abovementioned method in addition to certain concentration of TPGS-PTX NC or GNRs and stored at 4°C. GNRs-TPGS-PTX NC-gels were prepared simply by mixing the TPGS-PTX NC-gel, GNRs-gel, and blank gel solution before use according to the required concentration of drug and GNRs.

Characterization of the GNRs-TPGS-PTX NC-gel system

Zeta potential and morphology

The zeta potential of CTAB-GNRs and PEG-GNRs was measured using a Zetasizer (Nano ZS90; Malvern Instruments, Malvern, UK) at 25°C in water. The absorption spectrum was scanned with a Microplate reader (Thermo Scientific™ Multiskan™ GO; Thermo Fisher Scientific, Waltham, MA, USA). Transmission electron microscopy (TEM) was performed on a Hitachi HT7700 microscope (Hitachi Ltd., Tokyo, Japan) to observe the shapes and size of CTAB-GNRs, PEG-GNRs, and TPGS-PTX NC. The Nano Measure software was used to measure their length and diameter. Inductively coupled plasma optical emission spectrometry was used to determine Au content of the GNRs.

Stability of PEG-GNRs

The stability of PEG-GNRs was assessed in either PBS or 10% FBS diluted with PBS to simulate a physiological condition. PEG-GNRs and CTAB-GNRs were incubated in PBS and 10% FBS, respectively. The concentration of Au for each solution was 60 μg mL^{-1}. The solutions were observed and photographed after 1 week.

Gel formation temperature (GFT) and gelation time (GT)

The tube inversion method was performed to determine the GFT and GT of various gels. The sample solution (1 mL) was added to the sample cell and observed while slowly heating the sample cell in a water bath at the range of 20°C–50°C. At each temperature point, the sample was equilibrated for a moment and visually observed by inverting the cell. The GFT was recorded at the point that no flow was observed when inverting the cell. The GT was measured by placing the sample solution in a 37°C water bath, and the time was recorded when the sample was placed into the water bath until it did not flow.

Rheological behavior of various gel systems

The rheological behavior of various gels was monitored using a dynamic shear rheometer (AR1500ex; TA Instruments, New Castle, DE, USA). The sample was placed on a parallel plate with a temperature controller. A thin layer of silicon oil was added to the outer edge of the sample to prevent evaporation of the solvent. The storage modulus (G′) and the loss modulus (G″) were recorded when the temperature changed. The temperature was increased from 20°C to 50°C at an interval of 1°C. The parameters of rheological assay were set as the controlled strain γ of 0.4%, angular frequency of 1 rad s^{-1}, and equilibration time of 90 seconds.

Evaluation of photothermal conversion

To evaluate the photothermal conversion efficiency of PEG-GNRs, 1 mL of GNRs-TPGS-PTX NC-gel sample (2 mg PTX mL^{-1}) with different Au concentrations (0, 10, 15, 20, 30 μg mL^{-1}) was irradiated by 808 nm NIR laser with an intensity of 2 W cm^{-2}. The temperature change was monitored by an infrared thermal imager (VarioCAM® HD; InfraTec GmbH, Dresden, Germany) for 25 minutes at an interval of 1 minute per time.

In vitro drug release

The in vitro drug release was measured using a dialysis method. F127-PTX NC-gel, TPGS-PTX NC-gel, GNRs-TPGS-PTX NC-gel, and GNRs-TPGS-PTX NC-gel were sealed in dialysis bags (MW cutoff: 8–14 kDa) and immersed into 20 mL of sodium salicylate solution (1.0 M) at 37°C with gentle shaking (100 rpm) for 144 hours. At each time point,

5 mL of the media outside the dialysis bags was withdrawn and replaced with an equal volume of pre-warmed fresh media. To study the effects of NIR light on the drug release behavior, GNRs-TPGS-PTX NC-gels were exposed to an NIR laser at 808 nm, 2 W cm^{-2} for 5 minutes at each time point. To determine the concentration of PTX, each sample was diluted with methanol and centrifuged to remove PEG-GNRs and quantified using an HPLC with an ultraviolet detector (HPLC-UV, Agilent 1260). The column was an octadecylsilyl column (Eclipse XDB-C18, 5 μm, 250×4.6 mm). The injection volume was 20 μL, and the detection wavelength was set at 230 nm. The solvent mobile phase was 56% acetonitrile and 44% water at a flow rate of 1 mL min^{-1}. The elution time for PTX was ~7.2 minutes.

In vitro erosion

The erosion experiments of the five types of gel systems (blank, TPGS-PTX NC-gel, GNRs-gel, GNRs-TPGS-PTX NC-gel, and GNRs-TPGS-PTX NC-gel with laser) were performed in vitro. The concentration of PTX was set as 2.5 mg mL^{-1} for each sample. The gel (1 mL per sample) in the solution state was placed into the test tube with a diameter of 1 cm and incubated in a water bath at 37°C until gel formed. Then, 2 mL of pre-warmed PBS (0.01 M) was cautiously added to the surface of the gel, and the test tube was placed in a constant temperature shaker at a rate of 100 rpm and the temperature of 37°C. Samples in GNRs-TPGS-PTX NC-gel with the laser group were irradiated by an NIR laser at 808 nm (2 W cm^{-2}, 10 minutes), The samples were photographed, and the gel interfaces were measured at predetermined time points.

Cell line and cell culture

The parental cell line SW620 is a human colon cell line that originated from a lymph node metastasis in the patient with a primary adenocarcinoma of the colon. SW620 and its drug-selected P-gp-overexpressing SW620 AD300 subline were provided by Dr Susan E Bates (Columbia University, New York, NY, USA). The use of the cell line has been approved by the institutional review board of Tianjin Medical University. These cells were cultured in DMEM supplemented with 10% FBS and 1% penicillin/streptomycin and incubated at 37°C in a humidified atmosphere with 5% CO_2. All cells were grown as adherent monolayers in drug-free culture media for more than 2 weeks before assays.

Cytotoxicity assay

The MTT colorimetric assay was used to evaluate the drug resistance of the cells and to detect the cytotoxicity of different formulations. Cells were seeded into a 96-well plate at 8,000 cells/well and cultured overnight to allow the cells to attach. Different concentrations of drugs (100 μL/well) were then added into the designated wells. To measure the photothermal effect, wells containing PEG-GNRs were irradiated by an NIR laser (808 nm, 2 W cm^{-2}) for 2 minutes. After a 24- or 72-hour incubation, 20 μL of MTT (5 mg mL^{-1}) was added to each well, and the plate was further incubated at 37°C for 4–6 hours, allowing viable cells to change the yellow-colored MTT to dark blue formazan crystals. Then, the medium was carefully discarded, and 200 μL of dimethyl sulfoxide was added to each well to dissolve the crystals. Plates were placed on a shaking table to thoroughly mix the formazan into the solvent. Finally, the absorbance was determined at 490 nm by a Microplate reader. The IC_{50} values of each formulation were determined by Prism 4.0 (Graphpad Software; GraphPad Software, Inc., La Jolla, CA, USA). According to the previous reports, the degree of resistance was calculated by dividing the IC_{50} of the SW620 AD300 cells by that of the parental cell SW620.[29] The degree of the reversal of MDR was calculated by dividing the IC_{50} value of SW620 AD300 cells with the anticancer drug in the absence of TPGS by that obtained in the presence of TPGS.[30]

The in vivo NIR photothermal images

Male Nu/Nu nude mice (18–25 g) were used for the in vivo infrared thermal images. Drug-resistant SW620 AD300 cells (5×10^6) in 100 mL of PBS were injected subcutaneously in the groin of mice. Tumor growth was monitored every other day until tumor volume reached ~100 mm^3. The whole-body infrared thermal images of the mice receiving the treatment of PBS, GNRs-gel, or GNRs-TPGS-PTX NC-gel, which were irradiated at 808 nm at an intensity of 2 W cm^{-2}, were captured using an infrared thermal imager at 0, 1, 3, and 5 minutes during the laser irradiation.

In vivo antitumor activity and systemic toxicity

The SW620 AD300 tumor-bearing mice were randomly divided into four groups of eight mice per group. Each group of animals received a single peritumoral injection of 200 μL of PBS, TPGS-PTX NC-gel, GNRs-gel, or GNRs-TPGS-PTX NC-gel (PTX: 20 mg kg^{-1}; Au: 160 μg kg^{-1}). The 808 nm laser irradiation was carried out locally on the tumor of the GNRs-gel and GNRs-TPGS-PTX NC-gel groups at an intensity of 2 W cm^{-2} for 3 minutes on days 2 and 8 after gel administration. The tumor size of each mouse was recorded

every other day and calculated by the formula: $V = ab^2/2$ (a, length; b, width). The body weights of the animals were also measured every other day to determine treatment-relevant toxicities. At day 38 after the treatment, the mice were sacrificed, and their main organs (heart, liver, spleen, lung, and kidney) were collected and stained with H&E to observe organ toxicity. All the animal experiments were performed strictly in compliance with the requirements and guidelines of the institutional ethical committee of animal experimentation and approved by Tianjin Medical University Animal Care and Use Committee.

Statistical analyses

All values are expressed as mean ± SD of at least three independent experiments. Student's t-test was used to analyze the data, and a P-value of <0.05 was considered statistically significant.

Results and discussion

Characterization of PEG-GNRs

CTAB is a commonly used stabilizer in the preparation of the GNRs.[31] However, the high positive electric potential induces cytotoxicity by breaking up the lipid bilayer of the cell membranes.[32] In this study, mPEG-SH was used to substitute the CTAB surface and to improve the safety and biocompatibility of the GNRs. The typical morphologies, structures, and sizes of CTAB-GNRs and PEG-GNRs were analyzed by TEM (Figure 2A and B). TEM images confirm the rod shape of GNRs and show an average length of 45±5 nm and diameter of 12±2 nm (aspect ratio as defined by the length/diameter is 4–5) calculated by Nano Measure software. Absorption spectra of PEG-GNRs and CTAB-GNR solution were measured (Figure 2C). The absorption peak was around 795 and 802 nm for CTAB-GNRs and PEG-GNRs. After modification with PEG chains, a slight red shift was observed in duplicate tests; this indicated that the modification did not cause aggregation of particles.[33] The strong surface plasmon resonance of the PEG-GNRs in the NIR region indicated a good photothermal conversion property. The zeta potentials of the CTAB-GNRs and PEG-GNRs were 29.2±4.2 and −14.6±0.9 mV (Figure 2D), which demonstrated that mPEG-SH successfully replaced CTAB.

To further verify the stability of PEG-GNRs in physiological condition, CTAB-GNRs and PEG-GNRs were

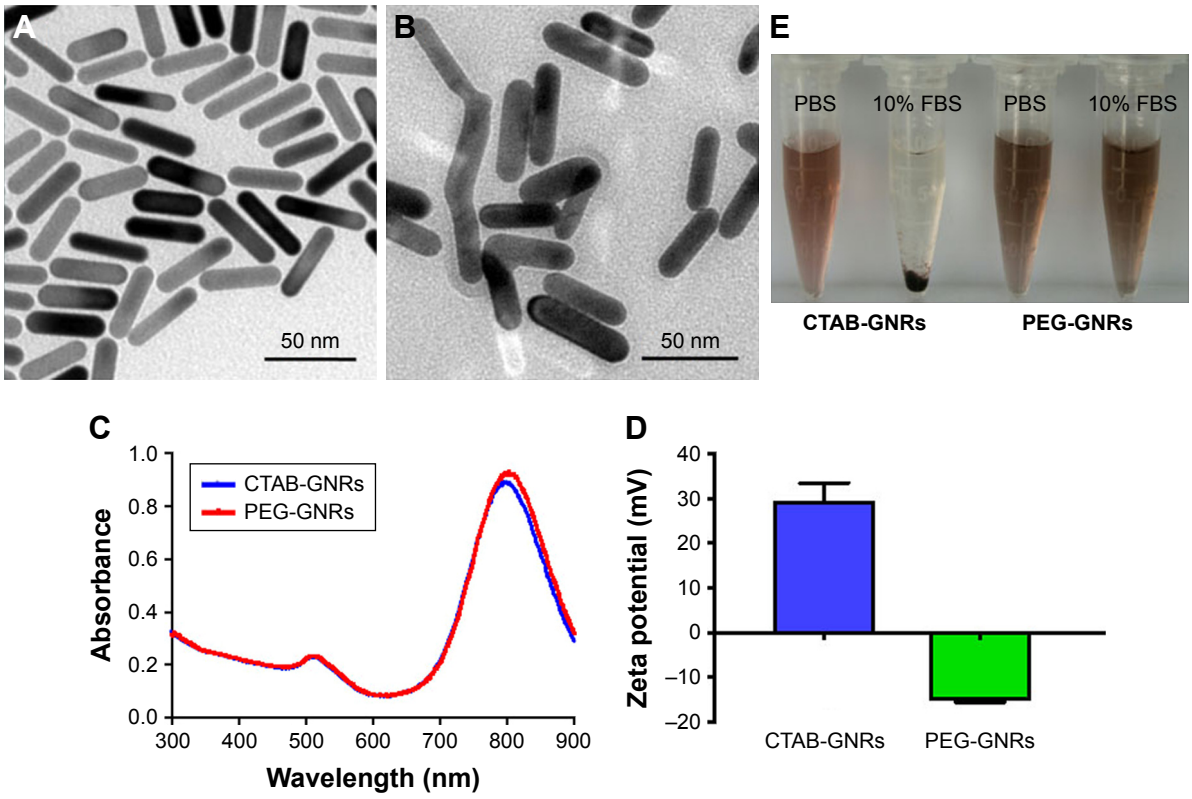

Figure 2 Characterization of PEG-GNRs.

Notes: TEM images of (**A**) CTAB-GNRs (×60K) and (**B**) PEG-GNRs (×80K). (**C**) Absorption spectra of CTAB-GNRs and PEG-GNRs (Au: 20 μg mL^{-1}). (**D**) Zeta potentials of CTAB-GNRs and PEG-GNRs (n=3). (**E**) The stability of CTAB-GNRs and PEG-GNRs in 10% FBS diluted with PBS or PBS, respectively. CTAB-GNRs, CTAB-coated GNRs; PEG-GNRs, PEG-coated GNRs.

Abbreviations: CTAB, hexadecyl trimethyl ammonium bromide; GNRs, gold nanorods; PEG, polyethylene glycol; TEM, transmission electron microscopy.

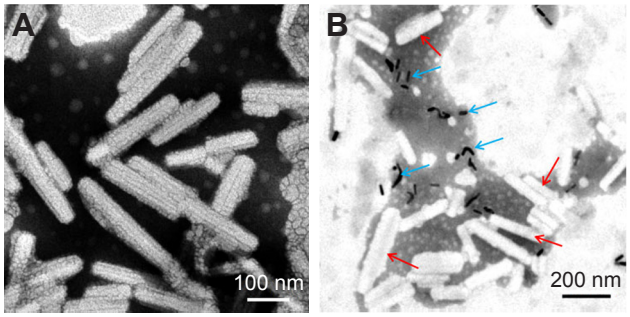

Figure 3 TEM images of (**A**) TPGS-PTX NC (×30K) and (**B**) GNRs-TPGS-PTX NC-gel (×15K; the red arrows represent TPGS-PTX NC; the blue arrows represent PEG-GNRs).
Notes: PEG-GNRs, PEG-coated GNRs; TPGS-PTX NC, TPGS-coated PTX NC.
Abbreviations: GNRs, gold nanorods; NC, nanocrystal; PEG, polyethylene glycol; PTX, paclitaxel; TEM, transmission electron microscopy; TPGS, D-alpha-tocopheryl PEG 1000 succinate.

placed in either 10% FBS diluted with PBS or plain PBS solution. After a week, the CTAB-GNRs showed precipitation in 10% FBS solution, while PEG-GNRs dispersed well in it. This indicated that PEG-GNRs have higher stability than CTAB-GNRs in physiological conditions with the presence of serum protein (Figure 2E).

Morphology and particle size of TPGS-PTX NC and GNRs-TPGS-PTX NC-gel

TPGS-PTX NC was prepared using TPGS as the sole excipient. PTX formed the NC, and TPGS was coated on the surface of the NC. As shown in Figure 3A, TPGS-PTX NC exhibits a rod shape with a length of ~150–300 nm and a width of about 40 nm.

The gel was prepared by combining different ratios of F127 and F68. The GFT and GT values of the gel were optimized by adjusting the ratio of F127 and F68, ensuring the gel injected into the body in a liquid state and followed by a quick gelation at body temperature to achieve local retention and controlled release of the loaded drugs. The final formulation of the gel was 22.5% F127 and 2.5% F68 with GFT of 31.2°C±0.4°C and GT of 78.3±5.7 seconds (Tables S1 and S2). From the TEM image of GNRs-TPGS-PTX NC-gel, both short rod-shaped TPGS-PTX NC and PEG-GNRs were observed (Figure 3B), which suggested that both the TPGS-PTX NC and PEG-GNRs were loaded into the gel and their particle size and morphology did not change significantly after being loaded into the gel.

Thermal sensitivity of the GNRs-TPGS-PTX NC-gel

The thermosensitive gel undergoes reversible sol–gel transition above LCST. To test the sol–gel transition property of the gel, the tube inversion method was used to roughly measure the GFT and GT of different gels. Table 1 summarizes the GFT and GT values of four thermosensitive gels. GFT was ~30°C for all the formulations. The GT values of blank group, F127-PTX NC-gel, and TPGS-PTX NC-gel were about 70–80 seconds. However, the GT values of GNRs-TPGS-PTX NC-gel decreased to about 50 seconds. The shorter GT benefits the administration of gel system in vivo, since the gel will transform from solution to gel state more quickly after injection for better local retention and controlled release of loaded drugs.[23]

The thermoresponsive sol–gel phase transition behavior of different gel systems was further investigated by monitoring their storage modulus (G′) and loss modulus (G″) via dynamic shear rheometer. The storage modulus G′ provides information regarding the elasticity or energy stored in the material during deformation, whereas the loss modulus G″ describes the viscous character or energy that dissipates with increasing temperature. The GFT was identified as the temperature at which the G′ and G″ curves crossed each other.[34] As shown in Figure 4A–D, G′ was lower than G″ before the crossover but higher than G″ after the crossover, suggesting that the sol–gel transition occurred at the crossover temperature between G′ and G″ curves. The GFTs of blank gel, F127-PTX NC-gel, TPGS-PTX NC-gel, and GNRs-TPGS-PTX NC-gel were about 31.5°C, 29.0°C, 29.4°C, and 27.6°C, respectively. This result was consistent with the data given in Table 1. Meanwhile, G′ and G″ indicated the viscoelastic behavior change of gels with temperature. At temperature below GFT, the gel had a more viscous behavior and could be easily injected in vivo. However, its elasticity was more significant when the temperature was above the GFT, forming a good coverage and retention at tumor site in vivo. The results showed that the

Table 1 GFT and GT of different gels (n=4)

	Blank	F127-PTX NC-gel	TPGS-PTX NC-gel	GNRs-TPGS-PTX NC-gel
GFT (°C)	31.2±0.4	28.4±0.3	28.2±0.2	28.3±0.3
GT (seconds)	78.3±5.7	80.0±2.7	73.8±8.5	49.5±0.8

Abbreviations: GFT, gel formation temperature; GNRs, gold nanorods; GT, gelation time; NC, nanocrystal; PEG, polyethylene glycol; PTX, paclitaxel; TPGS, D-alpha-tocopheryl PEG 1000 succinate.

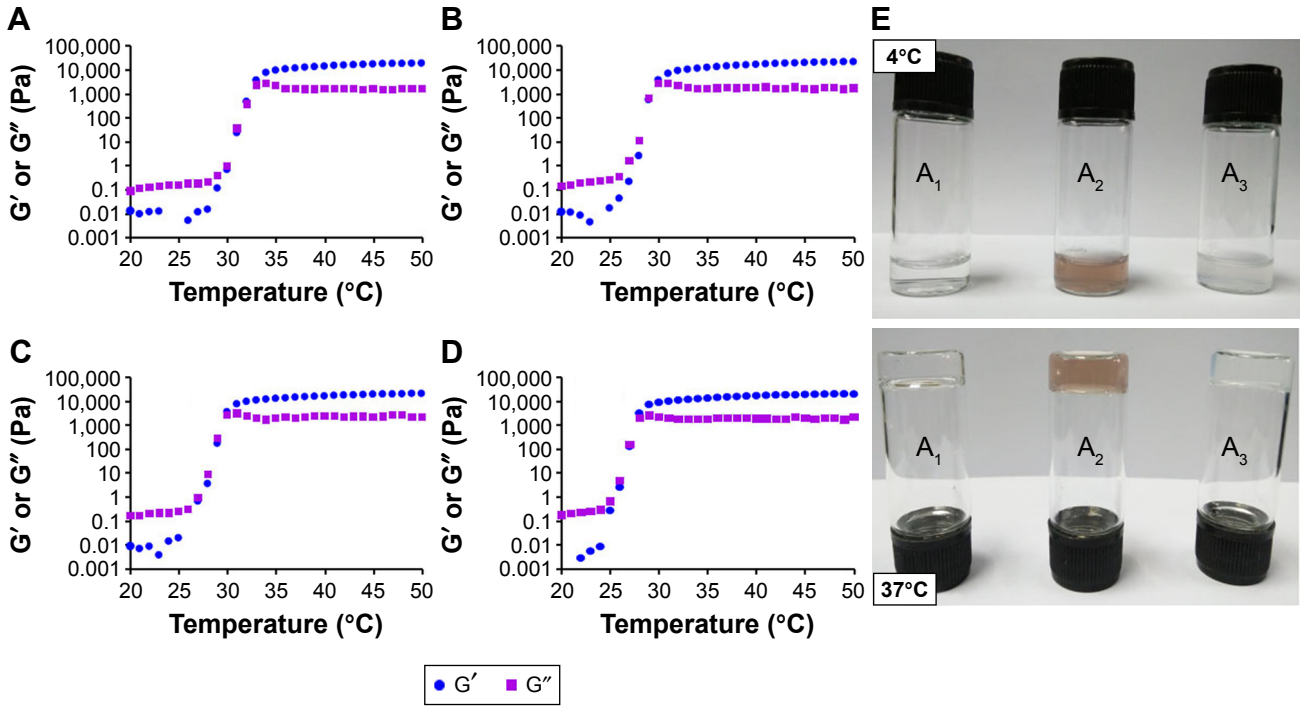

Figure 4 Storage modulus (G′) and loss modulus (G″) changes of gel with temperature from 20°C to 50°C. (**A**) Blank; (**B**) F127-PTX NC-gel; (**C**) TPGS-PTX NC-gel; (**D**) GNRs-TPGS-PTX NC-gel. (**E**) Photographs of various gels at different temperatures; (A_1) F127-PTX NC-gel, (A_2) GNRs-TPGS-PTX NC-gel, and (A_3) TPGS-PTX NC-gel.
Abbreviations: GNRs, gold nanorods; NC, nanocrystal; PEG, polyethylene glycol; PTX, paclitaxel; TPGS, D-alpha-tocopheryl PEG 1000 succinate.

sol–gel transition was moderate, making the gel suitable for manipulation in vitro and application in vivo.

Figure 4E shows the appearance of various gels at different temperatures. Soluble state was observed at a low temperature of 4°C. When the temperature was raised to 37°C, a semisolid state was observed. From the abovementioned GFT and GT measurement experiments (Table 1) and rheological experiments and morphology (Figure 4) experiments, we can conclude that the GNRs-TPGS-PTX NC-gel exhibited a sol–gel transition at around 28.3°C in about 50 seconds, suitable for in vivo injections followed by creating a viscous in situ gel for drug's retention at local site and sustained release.

Photothermal effect of the GNRs-TPGS-PTX NC-gel

Different concentrations of PEG-GNRs were incorporated into the gels, and the gel was irradiated with an 808 nm NIR light at 2 W cm^{-2} for 25 minutes. As shown in Figure 5A,

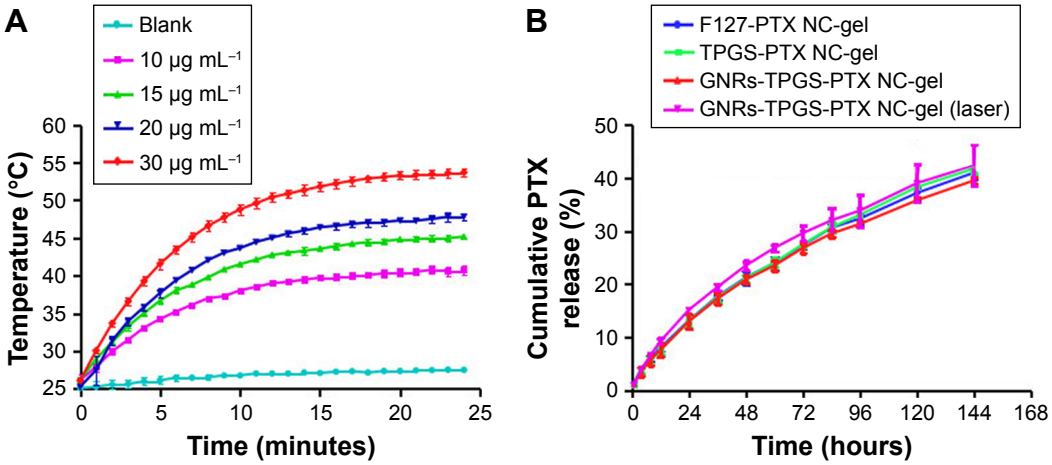

Figure 5 The photothermal efficacy and in vitro drug release of the gel.
Notes: (**A**) Temperature change of GNRs-TPGS-PTX NC-gel at various Au element concentrations during NIR laser irradiation for 25 minutes. (**B**) In vitro release of PTX from gel at 37°C. Laser irradiation (808 nm, 2 W cm^{-2}, 5 minutes). The results represent mean ± SD (n=3).
Abbreviations: GNRs, gold nanorods; NC, nanocrystal; NIR, near-infrared; PEG, polyethylene glycol; PTX, paclitaxel; TPGS, D-alpha-tocopheryl PEG 1000 succinate.

both the increasing rate and the final temperature of the gels were dependent on the Au content. The higher Au content correlated with a faster heating rate and a higher final stable temperature. Within 5 minutes of irradiation, the temperature of the formulation with Au element concentration of 30 μg mL^{-1} increased by 16.9°C (from 25.1°C to 42.0°C), which could induce cell death. Conversely, the blank gel only increased by about 2.4°C after being irradiated for 25 minutes. The results indicated that the PEG-GNRs could rapidly and efficiently convert NIR light into thermal energy. The photothermal effect could be easily adjusted by adding different concentrations of PEG-GNRs into the gel according to patient-specific factors.

In vitro drug release of the GNRs-TPGS-PTX NC-gel

The in vitro drug release of the GNRs-TPGS-PTX NC-gel was displayed by a dynamic dialysis method. Sodium salicylate (1.0 M in purified water) was used as the medium to achieve a sink condition of PTX.[35] As shown in Figure 5B, GNRs-TPGS-PTX NC-gel exhibited a slow and sustained release of PTX without the burst release effect. PTX release was quantified for 6 days, and the final cumulative release amount of PTX was up to 40%. Neither blending of GNRs into the gel nor the laser irradiation affected the release profile of PTX. The long-term sustained release profile of PTX was attributed to the slow dissolution of NC and the gel barrier effect,[36] which would serve as a depot for PTX after injection and reduce the toxicity of high-dose PTX to healthy tissues around the injection site.

In vitro erosion of the GNRs-TPGS-PTX NC-gel

To understand the erosion of the gels after injection, the in vitro erosion experiment was performed. As shown in Figure 6, all the gel interfaces declined slowly during the first 10 days, but quickly declined in 10–18 days. This implied that the gel first swelled because of water absorption and then slowly eroded. In addition, there was no significant difference in erosion rate between all the gel systems.

Cytotoxicity studies

First, the drug-resistant property of SW620 AD300 cells was tested. SW620 cells and SW620 AD300 cells were treated with different concentrations of PTX for 24 or 72 hours. As shown in Figures 7A and B and 8A and B, the

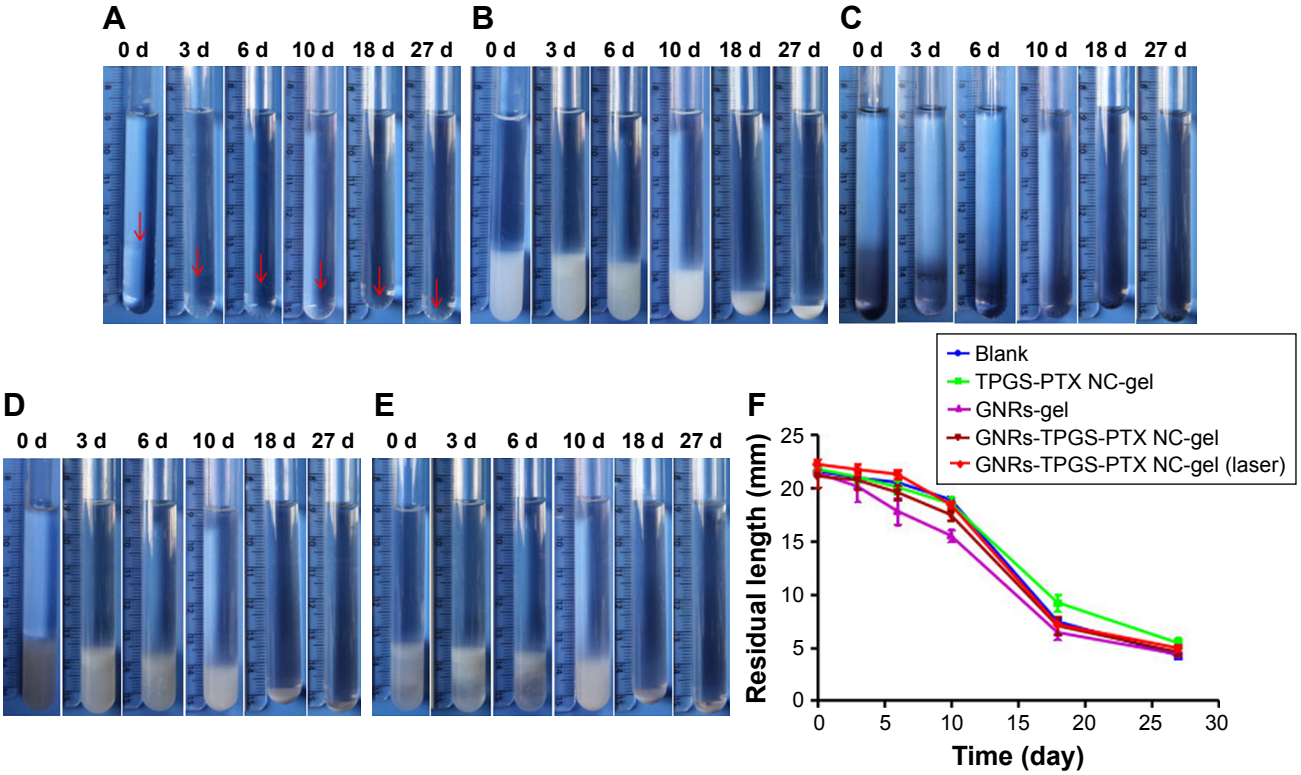

Figure 6 Photographs during gel erosion in vitro.
Notes: At various time points, the tubes were photographed by a digital camera. (**A**) Blank; (**B**) TPGS-PTX NC-gel; (**C**) GNRs-gel; (**D**) GNRs-TPGS-PTX NC-gel; (**E**) GNRs-TPGS-PTX NC-gel (laser). (**F**) The height of the remaining gel in the tube. Arrows imply gel formulation interfaces (n=3).
Abbreviations: d, days; GNRs, gold nanorods; NC, nanocrystal; PEG, polyethylene glycol; PTX, paclitaxel; TPGS, D-alpha-tocopheryl PEG 1000 succinate.

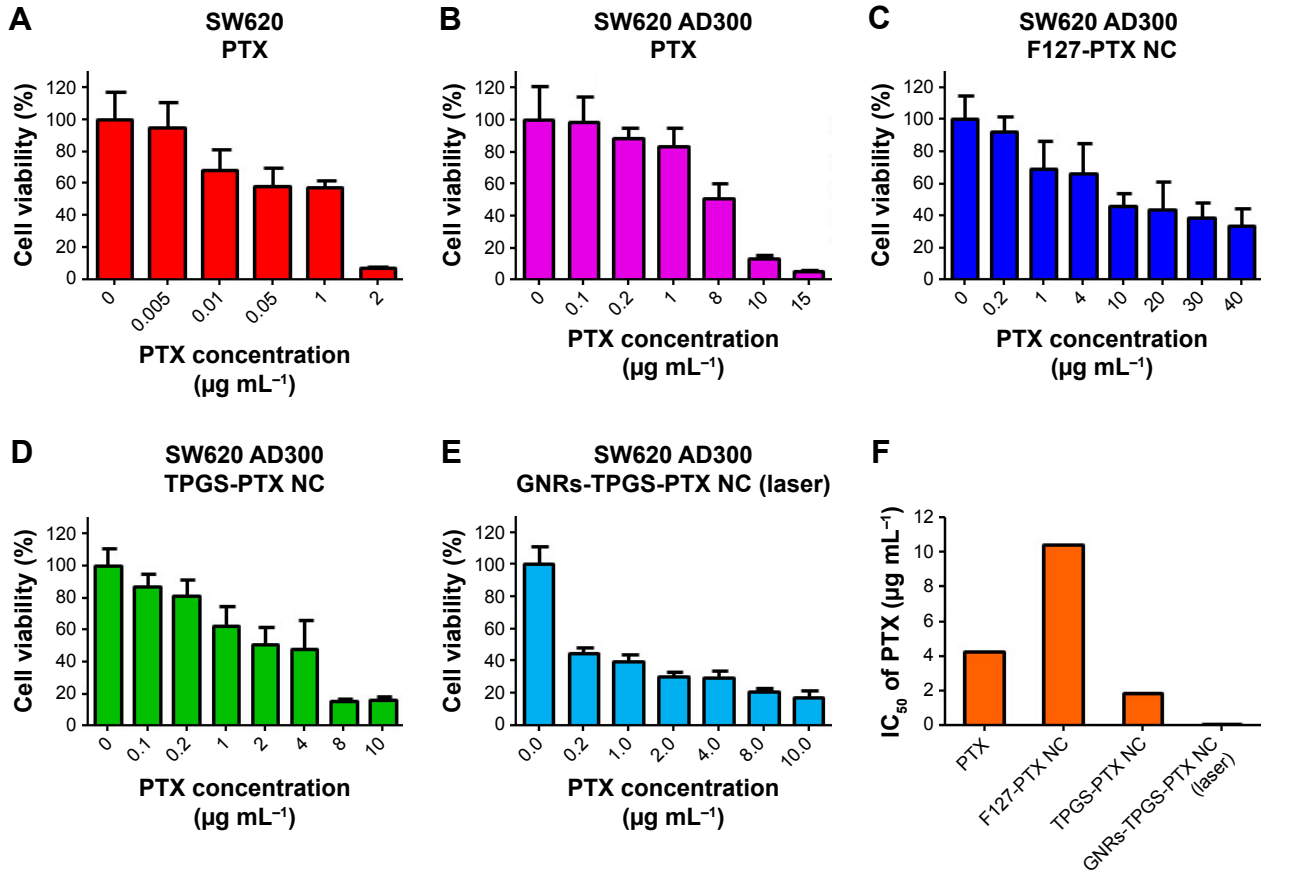

Figure 7 In vitro cytotoxicity assessments by MTT assay in SW620 and SW620 AD300 cells after treatment for 24 hours.
Notes: (**A**) The inhibitory effects of PTX on the proliferations of SW620 cells. Cytotoxicities of PTX (**B**), F127-PTX NC (**C**), TPGS-PTX NC (**D**), and GNRs-TPGS-PTX NC (**E**) in SW620 AD300 cells (n=6). (**F**) IC_{50} values of PTX of different formulations against SW620 AD300 cells. TPGS-PTX NC, TPGS-coated PTX NC.
Abbreviations: GNRs, gold nanorods; NC, nanocrystal; PEG, polyethylene glycol; PTX, paclitaxel; TPGS, D-alpha-tocopheryl PEG 1000 succinate.

sensitivities to PTX were very different between SW620 cells and SW620 AD300 cells. The IC_{50} values of PTX against SW620 and SW620 AD300 cells were 0.201 and 4.271 μg mL^{-1} after 24 hours and 0.015 and 1.601 μg mL^{-1} after 72 hours of the drug treatment (Tables 2 and 3). The resistance index (calculated by dividing the IC_{50} of SW620 AD300 by SW620 cells) of PTX for SW620 AD300 cells was about 107 after treatment for 72 hours, which was higher than that of the treatment for 24 hours. The result indicated that the drug resistance of SW620 AD300 cells was more remarkable when the treatment time extended.

To investigate the cytotoxicity of F127-PTX NC, TPGS-PTX NC, and GNRs and TPGS-PTX NC mixture, MTT assays were performed using SW620 AD300 cells. The anticancer efficacy was quantified by IC_{50} value (Table 3 and Figures 7F and 8F). In the 24-hour test, the cytotoxicity of TPGS-PTX NC (IC_{50} 1.880 μg mL^{-1}) was higher than that of PTX (IC_{50} 4.271 μg mL^{-1}), whereas that of F127-PTX NC (IC_{50} 10.40 μg mL^{-1}) was lower than that of PTX (IC_{50} 4.271 μg mL^{-1}; Figure 7B–D). When the incubation time was extended for 72 hours, the cytotoxicity of TPGS-PTX NC (IC_{50} 0.403 μg mL^{-1}) was more significantly enhanced compared with PTX (IC_{50} 1.601 μg mL^{-1}) and F127-PTX NC (IC_{50} 1.998 μg mL^{-1}; Figure 8B–D). The results indicated that TPGS-PTX NC could enhance the cytotoxicity of PTX in drug-resistant tumor. This is mainly because TPGS inhibits the ATPase activity of P-gp, thus decreasing the efflux of PTX, resulting in more drug accumulation inside the cells.[37,38] Moreover, even though TPGS-PTX NC significantly increased the cytotoxicity of PTX in drug-resistant SW620 AD300 cells, it could not reverse drug resistance, as the IC_{50} value is still much higher than PTX in SW620 cells. For the combination of chemotherapy and PTT, GNRs (5 μg mL^{-1}) were added into the culture medium, which were then irradiated with laser (2 W cm^{-2}, 2 minutes). As shown in Figures 7E and 8E, the IC_{50} values of GNRs combined with TPGS-PTX NC were much lower than those of the other two formulations (F127-PTX NC and TPGS-PTX NC) on SW620 AD300 cells and even lower than the IC_{50} value of SW620 cells. These results demonstrated that the combination of chemotherapy

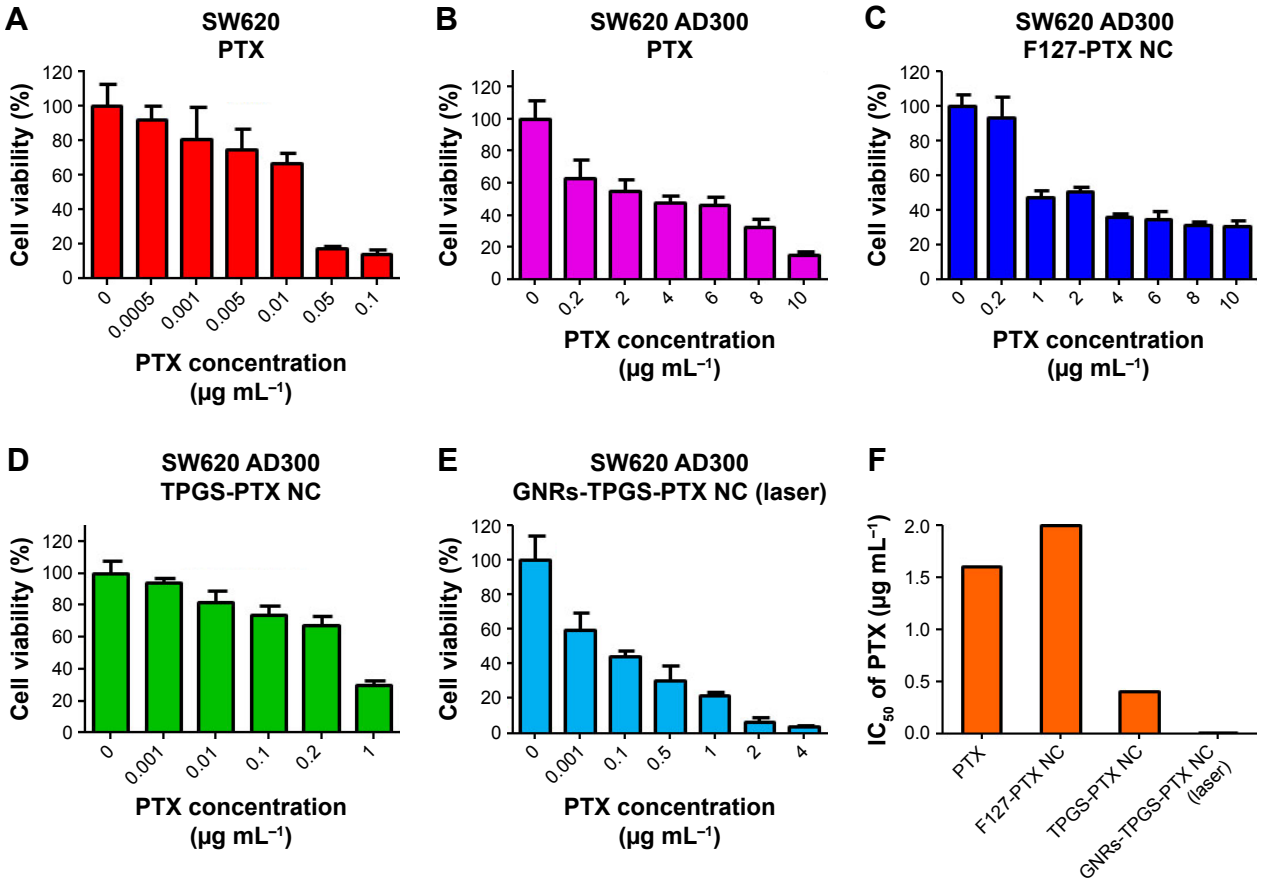

Figure 8 In vitro cytotoxicity assessments by MTT assay in SW620 and SW620 AD300 cells after treatment for 72 hours.
Notes: (**A**) The inhibitory effects of PTX on the proliferations of SW620 cells. Cytotoxicities of PTX (**B**), F127-PTX NC (**C**), TPGS-PTX NC (**D**), and GNRs-TPGS-PTX NC (**E**) in SW620 AD300 cells (n=6). (**F**) IC_{50} values of PTX of different formulations against SW620 AD300 cells. TPGS-PTX NC, TPGS-coated PTX NC.
Abbreviations: GNRs, gold nanorods; NC, nanocrystal; PEG, polyethylene glycol; PTX, paclitaxel; TPGS, D-alpha-tocopheryl PEG 1000 succinate.

and PTT via TPGS-PTX NC and GNRs exhibited a strong synergistic cytotoxic effect against SW620 AD300 cells and reversed the MDR of PTX.

The in vivo photothermal imaging

Encouraged by the effectiveness of GNR-induced photothermal ablation of SW620 AD300 cancer cells in vitro, the in vivo photothermal efficacy of the gel platforms was further investigated in SW620 AD300 tumor-bearing mice using 808 nm laser exposures with an intensity of 2 W cm^{-2}. First, the local tumor temperature changes were monitored at different time points by an infrared thermal camera (Figure 9). We chose the irradiation condition of 2 W cm^{-2}, 3 minutes for the animal efficacy study, in which the average temperature in the tumor region of the PBS group is 40.68°C±0.25°C. According to the previous reports, in this condition, NIR irradiation does not cause systemic side effect, and the skin injury at the location of laser exposure was reversible.[13,39] The average temperature in the tumor region of the GNRs-gel and GNRs-TPGS-PTX NC-gel groups was 48.18°C±4.25°C and 47.35°C±3.56°C, respectively, which was high enough to kill tumor cells in vivo.[40] The surrounding tissue near the tumor showed a slight temperature increase to 35°C–40°C, and no significant temperature change was observed on other parts of the mice, which indicated that PTT did not exert damage either to the local healthy tissues or the whole body. This result demonstrated that GNRs-TPGS-PTX NC-gel could exert efficient local PTT in vivo without damaging surrounding healthy tissues.

Table 2 IC_{50} values of SW620 cells after PTX administration at 24- or 72-hour incubation time (n=6)

Incubation time	PTX (μg mL^{-1})
24 hours	0.201 (0.006–6.925)
72 hours	0.015 (0.008–0.027)

Note: The numbers in parentheses represent 95% CIs of IC_{50}.
Abbreviation: PTX, paclitaxel.

The in vivo antitumor efficacy

The in vivo therapeutic efficacy and systemic toxicity of the various gel systems were studied on SW620 AD300

Table 3 IC_{50} values of SW620 AD300 cells and reversal index after treatment with different formulations at 24- or 72-hour incubation time (n=6)

	24 hours (μg mL^{-1})	Reversal index	72 hours (μg mL^{-1})	Reversal index
PTX	4.271 (1.466–12.44)	1.000	1.601 (0.325–7.878)	1.000
F127-PTX NC	10.40 (6.682–16.19)	0.411	1.998 (1.070–3.730)	0.801
TPGS-PTX NC	1.880 (1.128–3.133)	2.272	0.403 (0.136–1.197)	3.973
GNRs-TPGS-PTX NC	0.141 (0.038–0.519)	30.29	0.009 (0.0005–0.159)	177.9

Notes: The numbers in parentheses represent 95% CIs of IC_{50}. TPGS-PTX NC, TPGS-coated PTX NCs.
Abbreviations: GNRs, gold nanorods; NC, nanocrystal; PEG, polyethylene glycol; PTX, paclitaxel; TPGS, D-alpha-tocopheryl PEG 1000 succinate.

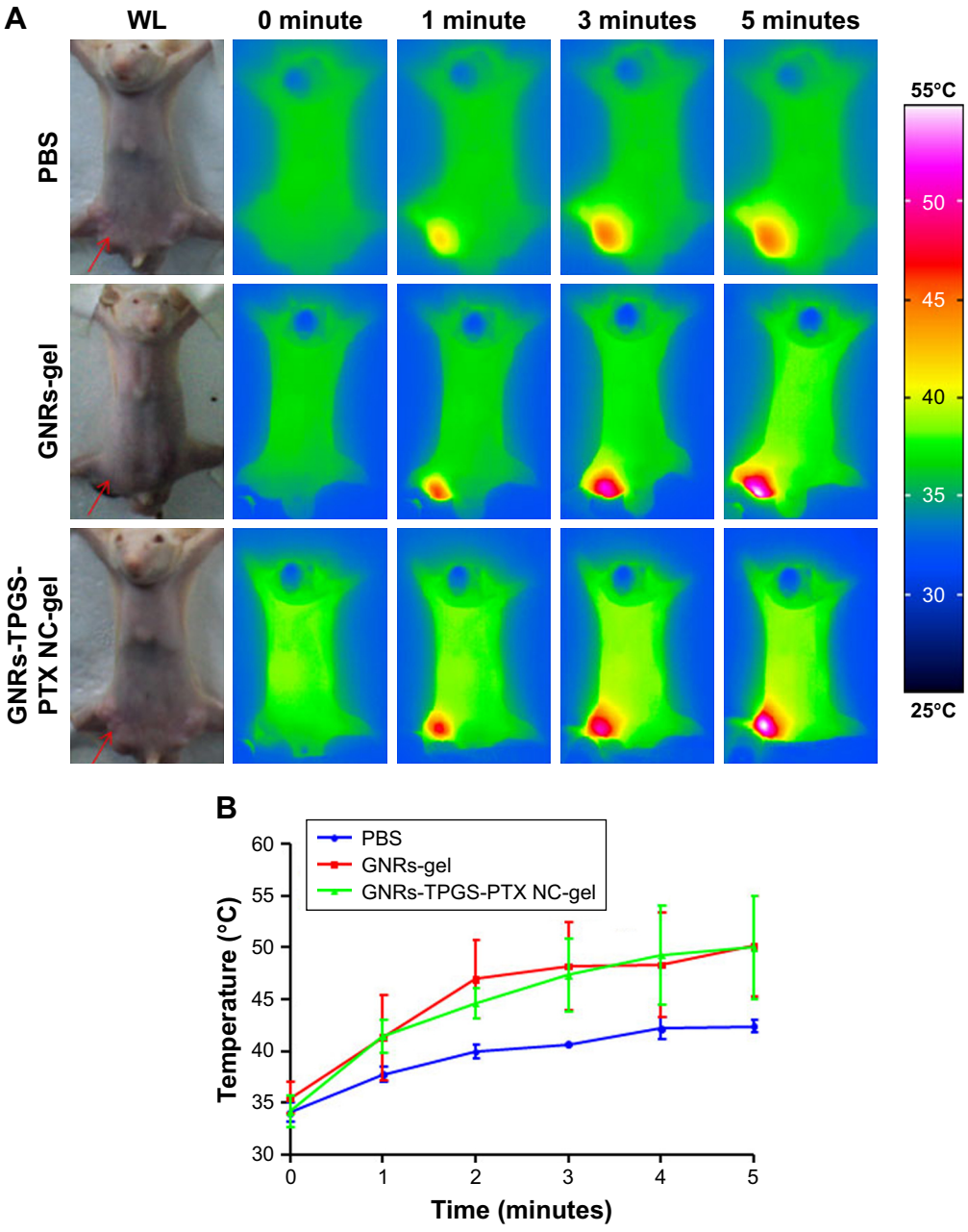

Figure 9 Infrared theamal images and average temperature changes at the tumor site over time.
Notes: (**A**) Infrared thermal images of tumors after 808 nm laser irradiation at 0, 1, 3, and 5 minutes in PBS-, GNRs-gel-, and GNRs-TPGS-PTX NC-gel-injected mice under 2 W cm^{-2} irradiation (the arrows represent the location of the tumor; WL). (**B**) The changes of average temperature in tumor region with time during NIR laser (808 nm, 2 W cm^{-2}) irradiation (n=2 for PBS group, n=3 for GNRs-gel and GNRs-TPGS-PTX NC-gel group).
Abbreviations: GNRs, gold nanorods; NC, nanocrystal; NIR, near-infrared; PEG, polyethylene glycol; PTX, paclitaxel; TPGS, D-alpha-tocopheryl PEG 1000 succinate; WL, white light.

tumor-bearing mice after peritumoral injection with PBS, TPGS-PTX NC-gel, GNRs-gel, and GNRs-TPGS-PTX NC-gel (PTX: 20 mg kg^{-1}; Au: 160 μg kg^{-1}). The GNRs-gel and GNRs-TPGS-PTX NC-gel groups were irradiated at 808 nm for 3 minutes at 2 W cm^{-2} on days 2 and 8. Compared with the rapid tumor growth of the control group, GNRs-gel with laser, TPGS-PTX NC-gel, and GNRs-TPGS-PTX NC-gel with laser groups all yielded tumor inhibitory effect but with a different extent (Figure 10A). In the first 14 days, GNRs-TPGS-PTX NC-gel with laser and GNRs-gel with laser exhibited significantly better efficacy than TPGS-PTX NC-gel alone, while GNRs-TPGS-PTX NC-gel with laser and GNRs-gel with laser showed similar efficacy (Figure 10B), suggesting that PTT played a more crucial role than chemotherapy at the early period of the treatment. However, as time extended, the tumor volume of GNRs-gel with the laser group increased more quickly than GNRs-TPGS-PTX NC-gel with the laser group, and a significant difference in tumor size between the two groups was achieved from day 22 until the end of the test. Similar results are shown in Figure 10C and D, in which GNRs-TPGS-PTX NC-gel with the laser group had the least tumor weight among the four groups; TPGS-PTX NC-gel and GNRs-gel with the laser groups showed similar tumor weight. The result indicated that using GNRs-gel with laser alone could control the tumor growth at the beginning, but tumors quickly recurred. On the contrary, with the combination of chemotherapy and PTT, GNRs-TPGS-PTX NC-gel with the laser group showed a much slower recurrence of the tumor and the smallest tumor volume among the three gel groups at the end of the test. The result is consistent with former reports, in which using chemotherapy combined with PTT reduced tumor recurrence and achieved better efficacy.[41] According to our previous work, after tumor local injection of PTX NC hydrogel system, PTX is mainly distributed in the tumor site from day 0 to 15.[20] Thus, the local delivery system allows the PTX to accumulate mostly in tumor to exert better therapeutic efficacy and less systemic toxicity comparing to intravenous injection. The controlled release pattern

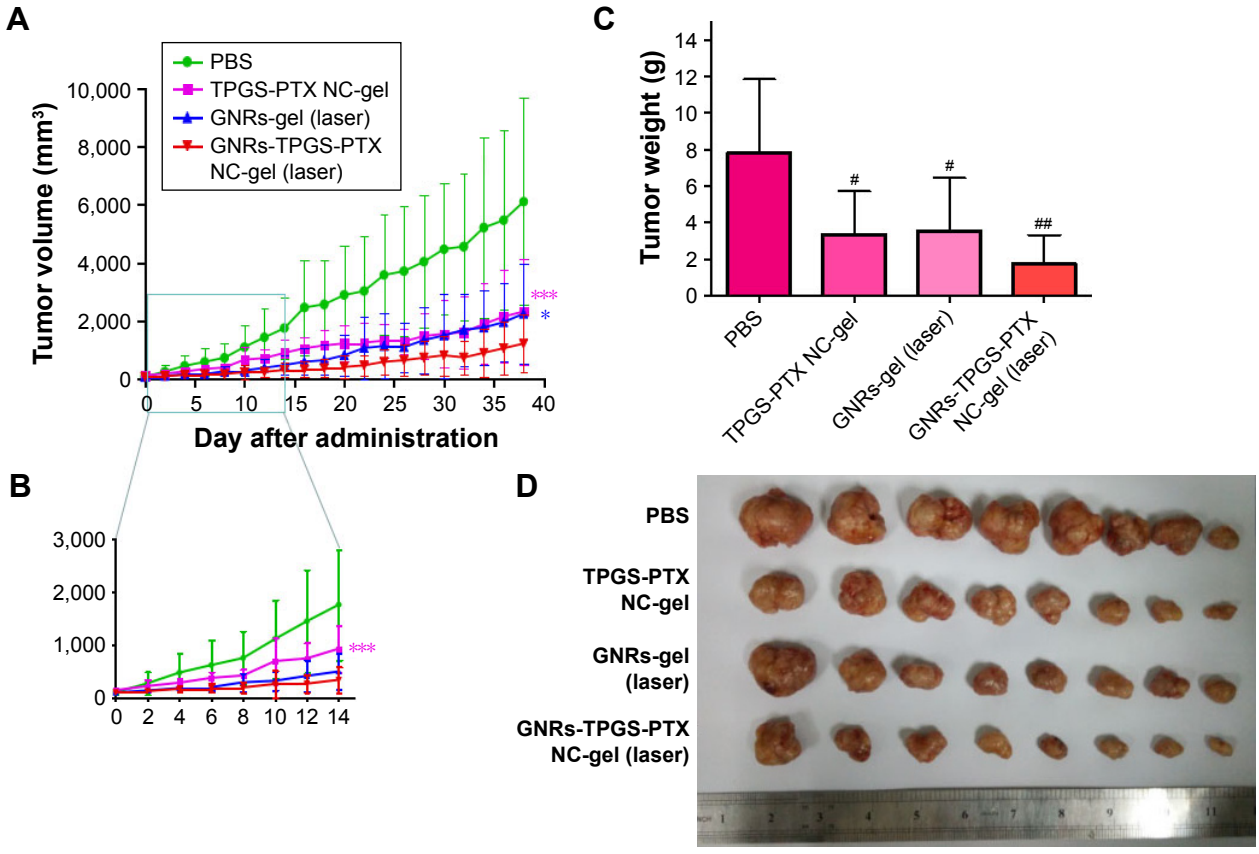

Figure 10 In vivo antitumor efficacy against SW620 AD300 tumor-bearing mice.
Notes: (**A**) Tumor volume growth of the tumor-bearing mice with different treatments (three purple *** represent the TPGS-PTX NC group, a blue * represents the GNRs-gel [laser] group). (**B**) Changes in tumor volume in each group in the first 14 days. (**C**) The mean weight of the excised SW620 AD300 tumors from the mice. (**D**) The images of excised tumors at the end of the treatment. ***$P<0.001$ and *$P<0.05$ vs the GNRs-TPGS-PTX NC-gel group. #$P<0.05$ and ##$P<0.01$ vs PBS group. Student's *t*-test was used to analyze the data and a *P*-value of <0.05 was considered statistically significant. The results represent mean ± SD (n=8). TPGS-PTX NC, TPGS-coated PTX NCs.
Abbreviations: GNRs, gold nanorods; NC, nanocrystal; PEG, polyethylene glycol; PTX, paclitaxel; TPGS, D-alpha-tocopheryl PEG 1000 succinate.

of TPGS-PTX NC might also contribute to the efficacy of combined therapy, since it will exert long-term efficacy to inhibit tumor recurrence after PTT.

Systemic toxicity studies

Systemic toxicity is always a great concern for chemotherapy; it can be reflected by animal weight loss and the histological variations of the main organs after treatment. The body weights of the animals were measured every other day during the treatment. As shown in Figure 11A, no significant body weight changes were observed in all the groups. To further evaluate the potential toxicity, major organs (heart, liver, spleen, lung, and kidney) from each group were analyzed by the H&E stain. No obvious organ damages and lesions were observed for all the groups (Figure 11B). These results indicated that the treatment of PTT and chemotherapy based on GNRs-TPGS-PTX NC-gel did not cause any serious side effects. Side effect is one of the major concerns for clinic translation of nanoplatform. To reduce the side effect of our nanoplatform, we used Food and Drug Administration (FDA)-approved excipients to make the PTX NC and hydrogel. In addition, PEG was used to substitute CTAB on the surface of GNRs to avoid the cytotoxicity of CTAB via breaking up the lipid bilayer of the cell membranes.[32] In consideration of the tolerance or safety of using gold nanoparticles in human beings, many studies have suggested that gold nanomaterials are bioinert and can be used safely.[42] Actually, gold has been used in clinics as anti-inflammatory and antirheumatic agents (Auranofin® [SKF, Gothenburg, Sweden] and Tauredon® [Byk Gulden, Wesel, Germany]) for decades. Recently, several gold nanoparticle-based therapeutic systems have entered into the clinic trials.[43] The PEGylated gold nanoparticle (27 nm) functionalized with rhTNF was administered systemically to 30 patients with advanced solid tumors, showing no detectable side effects (NCT00356980 and NCT00436410 from www.ClinicalTrials.gov). Silica–gold nanoshell (AuroLase® [Nanospectra Biosciences, Houston, TX, USA]) is the first gold nanoparticle-based photothermal therapeutic system which was approved by FDA for clinical study in treating solid tumor (NCT00848042 and NCT01679470 from www.ClinicalTrials.gov). The early clinical results show that the human body has a excellent tolerability to gold.[44] However, there are also some reports about the potential toxicities of gold nanoparticles in vivo. For example, some researchers have found that gold nanoparticles (10–50 nm) dispersed quickly to almost all tissues after intravenous injection, mainly accumulating in the liver, lung, spleen, and kidney at 24 hours post injection with potential toxicity to these organs. Although the gold nanoparticle is delivered at tumor site in our platform limiting its distributions to other tissues, more researches about

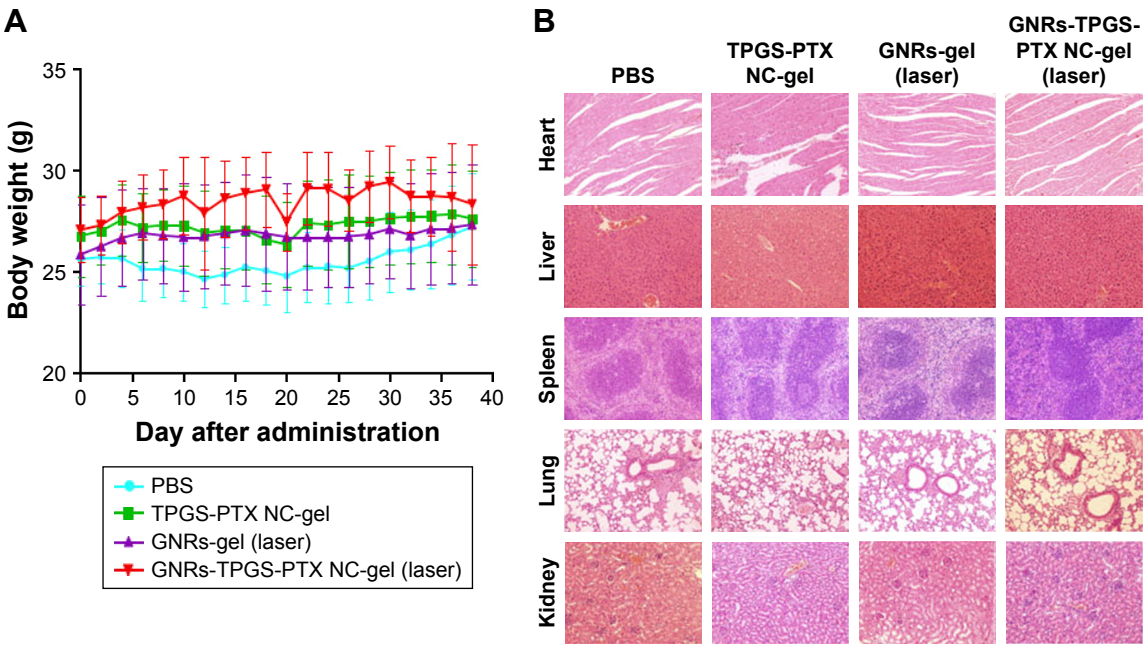

Figure 11 Systemic toxicity studies of the GNRs-TPGS-PTX NC-gel with laser.
Notes: (**A**) The body weight changes of SW620 AD300 tumor-bearing mice with different treatments (n=8). (**B**) H&E-stained images of major tissue sections including hearts, livers, spleens, lungs, and kidneys of mice after the treatments. The magnification used was 20×.
Abbreviations: GNRs, gold nanorods; NC, nanocrystal; PEG, polyethylene glycol; PTX, paclitaxel; TPGS, D-alpha-tocopheryl PEG 1000 succinate.

the fate of the gold nanoparticle as well as its long-term toxicity are needed in the future investigation.

The application of localized therapeutic system requires intratumoral injection; thus, it depends on cancer types. Previous researchers have demonstrated the clinical potential of local delivery system in several cancer types, such as lung, bronchus, breast, prostate, colon, rectum, urinary bladder, uterine corpus, and uterine cervix cancer.[45] Although surgery is the first choice for early-stage solid tumor, it is often associated with a high risk of recurrence and metastasis as well as many complications including bleeding at surgical sites, damaging to nearby organs, and leading to scar tissue and bowel obstruction along with tissue adhesions.[17] Systemic chemotherapy or radiotherapy is often used in clinics prior to surgical excision to shrink particularly large tumors, or after surgery to prevent recurrence and metastasis, but both therapies are related to acute and long-term toxicities.[45] In our study, the localized therapeutic system (GNRs-TPGS-PTX NC-gel system) provides a promising alternative to surgery by avoiding the pain and complications and preventing tumors from recurrence and metastasis or a potential neoadjuvant therapy used before or after surgery with limited side effects and well tolerance for patients. In the late stage of solid tumors, the localized nanoplatform can also serve as a palliative therapy for those unable to tolerate surgery.

Conclusion

In this study, a personalized and long-acting local therapeutic platform combining chemotherapy and PTT for the treatment of MDR CRC was successfully developed. After administration, the gel patch can first exert local PTT to shrink the tumor within 5 minutes without damaging surrounding healthy tissues; TPGS-PTX NC later provided a long-term sustained release of PTX to reduce the risk of local recurrence along with the P-gp inhibitor TPGS to reverse the drug resistance. The cytotoxicity studies showed that with the combination of chemotherapy and PTT the IC_{50} decreased to ~178-folds compared with PTX alone in drug-resistant SW620 AD300 cells. After one-time administration, the in vivo antitumor efficacy of GNRs-TPGS-PTX NC-gel with the laser group showed a much slower recurrence of the tumor compared with groups with PTT alone and with a significantly smaller tumor size after 38 days compared with other groups that used either chemotherapy or PTT alone. In addition, no obvious systemic toxicity was observed during the treatment, indicating a tolerable side effect profile and good biocompatibility. Overall, the GNRs-TPGS-PTX NC-gel may serve as a promising localized therapeutic system with the long-term efficacy to treat MDR CRC. Doses of PEG-GNRs and TPGS-PTX NC can be easily adjusted according to patient-specific factors before use, making it a potential personalized platform for future development.

Acknowledgments

This study was supported by the National Natural Science Foundation of China (grant no 81402857), the National Science Foundation of Tianjin city (grant no 17JCQNJC14100), and the China Postdoctoral Science Foundation (grant no 2016M590208). We thank Dr Susan E Bates for the SW620 and SW620 AD300 cell lines (Columbia University, New York, NY, USA).

Disclosure

The authors report no conflicts of interest in this work.

References

1. Siegel RL, Fedewa SA, Anderson WF, et al. Colorectal cancer incidence patterns in the United States, 1974–2013. *J Natl Cancer Inst*. 2017; 109(8):1–6.
2. Siegel RL, Miller KD, Fedewa SA, et al. Colorectal cancer statistics, 2017. *CA Cancer J Clin*. 2017;67(3):177–193.
3. Simmonds PC. Palliative chemotherapy for advanced colorectal cancer: systematic review and meta-analysis. Colorectal Cancer Collaborative Group. *BMJ*. 2000;321(7260):531–535.
4. Saltzman WM, Fung LK. Polymeric implants for cancer chemotherapy. *Adv Drug Deliv Rev*. 1997;26(2–3):209–230.
5. Shannon AM, Bouchier-Hayes DJ, Condron CM, Toomey D. Tumour hypoxia, chemotherapeutic resistance and hypoxia-related therapies. *Cancer Treat Rev*. 2003;29(4):297–307.
6. Szakács G, Paterson JK, Ludwig JA, Booth-Genthe C, Gottesman MM. Targeting multidrug resistance in cancer. *Nat Rev Drug Discov*. 2006; 5(3):219–234.
7. Krukiewicz K, Zak JK. Biomaterial-based regional chemotherapy: local anticancer drug delivery to enhance chemotherapy and minimize its side-effects. *Mater Sci Eng C Mater Biol Appl*. 2016;62:927–942.
8. Guo DD, Xu CX, Quan JS, et al. Synergistic anti-tumor activity of paclitaxel-incorporated conjugated linoleic acid-coupled poloxamer thermosensitive hydrogel in vitro and in vivo. *Biomaterials*. 2009; 30(27):4777–4785.
9. Chen Q, Wen J, Li H, Xu Y, Liu F, Sun S. Recent advances in different modal imaging-guided photothermal therapy. *Biomaterials*. 2016;106: 144–166.
10. Burke AR, Singh RN, Carroll DL, et al. The resistance of breast cancer stem cells to conventional hyperthermia and their sensitivity to nanoparticle-mediated photothermal therapy. *Biomaterials*. 2012;33(10):2961–2970.
11. Zhang Z, Wang J, Nie X, et al. Near infrared laser-induced targeted cancer therapy using thermoresponsive polymer encapsulated gold nanorods. *J Am Chem Soc*. 2014;136(20):7317–7326.
12. Lee SM, Kim HJ, Kim SY, et al. Drug-loaded gold plasmonic nanoparticles for treatment of multidrug resistance in cancer. *Biomaterials*. 2014;35(7):2272–2282.
13. Li L, Chen C, Liu H, et al. Multifunctional carbon-silica nanocapsules with gold core for synergistic photothermal and chemo-cancer therapy under the guidance of bimodal imaging. *Adv Funct Mater*. 2016;26(24): 4252–4261.
14. Cai X, Jia X, Gao W, et al. A versatile nanotheranostic agent for efficient Dual-mode imaging guided synergistic chemo-thermal tumor therapy. *Adv Funct Mater*. 2015;25(17):2520–2529.
15. Westermann AM, Jones EL, Schem BC, et al. First results of triple-modality treatment combining radiotherapy, chemotherapy, and hyperthermia for the treatment of patients with stage IIB, III, and IVA cervical carcinoma. *Cancer*. 2005;104(4):763–770.

16. Tian B, Wang C, Zhang S, Feng L, Liu Z. Photothermally enhanced photodynamic therapy delivered by nano-graphene oxide. *ACS Nano*. 2011;5(9):7000–7009.
17. Conde J, Oliva N, Zhang Y, Artzi N. Local triple-combination therapy results in tumour regression and prevents recurrence in a colon cancer model. *Nat Mater*. 2016;15(10):1128–1138.
18. Lu Y, Li Y, Wu W. Injected nanocrystals for targeted drug delivery. *Acta Pharm Sin B*. 2016;6(2):106–113.
19. Müller RH, Jacobs C, Kayser O. Nanosuspensions as particulate drug formulations in therapy. Rationale for development and what we can expect for the future. *Adv Drug Deliv Rev*. 2001;47(1):3–19.
20. Lin Z, Gao W, Hu H, et al. Novel thermo-sensitive hydrogel system with paclitaxel nanocrystals: high drug-loading, sustained drug release and extended local retention guaranteeing better efficacy and lower toxicity. *J Control Release*. 2014;174(1):161–170.
21. Bobo D, Robinson KJ, Islam J, Thurecht KJ, Corrie SR. Nanoparticle-based medicines: a review of FDA-approved materials and clinical trials to date. *Pharm Res*. 2016;33(10):2373–2387.
22. Lin Z, Xu S, Gao W, et al. A comparative investigation between paclitaxel nanoparticle- and nanocrystal-loaded thermosensitive PECT hydrogels for peri-tumoural administration. *Nanoscale*. 2016;8(44): 18782–18791.
23. Norouzi M, Nazari B, Miller DW. Injectable hydrogel-based drug delivery systems for local cancer therapy. *Drug Discov Today*. 2016; 21(11):1835–1849.
24. Jeong B, Kim SW, Bae YH. Thermosensitive sol-gel reversible hydrogels. *Adv Drug Deliv Rev*. 2002;54(1):37–51.
25. Ron ES, Bromberg LE. Temperature-responsive gels and thermogelling polymer matrices for protein and peptide delivery. *Adv Drug Deliv Rev*. 1998;31(3):197–221.
26. Liu Y, Yang F, Feng L, et al. *In vivo* retention of poloxamer-based *in situ* hydrogels for vaginal application in mouse and rat models. *Acta Pharm Sin B*. 2017;7(4):502–509.
27. Rowinsky EK. Paclitaxel (taxol). *New Engl J Med*. 1995;332(15): 1004–1014.
28. Zhu XM, Fang C, Jia H, et al. Cellular uptake behaviour, photothermal therapy performance, and cytotoxicity of gold nanorods with various coatings. *Nanoscale*. 2014;6(19):11462–11472.
29. Guo H, Liu Y, Wang Y, et al. pH-sensitive pullulan-based nanoparticle carrier for adriamycin to overcome drug-resistance of cancer cells. *Carbohydr Polym*. 2014;111(20):908–917.
30. Dai CL, Tiwari AK, Wu CP, et al. Lapatinib (Tykerb, GW572016) reverses multidrug resistance in cancer cells by inhibiting the activity of ATP-binding cassette subfamily B member 1 and G member 2. *Cancer Res*. 2008;68(19):7905–7914.
31. Hinman JG, Stork AJ, Varnell JA, Gewirth AA, Murphy CJ. Seed mediated growth of gold nanorods: towards nanorod matryoshkas. *Faraday Discuss*. 2016;191(10):9–33.
32. Connor EE, Mwamuka J, Gole A, Murphy CJ, Wyatt MD. Gold nanoparticles are taken up by human cells but do not cause acute cytotoxicity. *Small*. 2005;1(3):325–327.
33. Niidome T, Yamagata M, Okamoto Y, et al. PEG-modified gold nanorods with a stealth character for in vivo applications. *J Control Release*. 2006;114(3):343–347.
34. Chen YY, Wu HC, Sun JS, Dong GC, Wang TW. Injectable and thermoresponsive self-assembled nanocomposite hydrogel for long-term anticancer drug delivery. *Langmuir*. 2013;29(11):3721–3729.
35. Huh KM, Lee SC, Cho YW, Lee J, Jeong JH, Park K. Hydrotropic polymer micelle system for delivery of paclitaxel. *J Control Release*. 2005;101(1–3):59–68.
36. You J, Cao J, Zhao Y, Zhang L, Zhou J, Chen Y. Improved mechanical properties and sustained release behavior of cationic cellulose nanocrystals reinforced cationic cellulose injectable hydrogels. *Biomacromolecules*. 2016;17(9):2839–2848.
37. Collnot EM, Baldes C, Schaefer UF, Edgar KJ, Wempe MF, Lehr CM. Vitamin E TPGS P-glycoprotein inhibition mechanism: influence on conformational flexibility, intracellular ATP levels, and role of time and site of access. *Mol Pharm*. 2010;7(3):642–651.
38. Markman JL, Rekechenetskiy A, Holler E, Ljubimova JY. Nanomedicine therapeutic approaches to overcome cancer drug resistance. *Adv Drug Deliv Rev*. 2013;65(13–14):1866–1879.
39. von Maltzahn G, Park JH, Agrawal A, et al. Computationally guided photothermal tumor therapy using long-circulating gold nanorod antennas. *Cancer Res*. 2009;69(9):3892–3900.
40. Chen R, Zheng X, Qian H, Wang X, Wang J, Jiang X. Combined near-IR photothermal therapy and chemotherapy using gold-nanorod/chitosan hybrid nanospheres to enhance the antitumor effect. *Biomater Sci*. 2013; 1(3):285–293.
41. Nam J, Son S, Ochyl LJ, Kuai R, Schwendeman A, Moon JJ. Chemophotothermal therapy combination elicits anti-tumor immunity against advanced metastatic cancer. *Nat Commun*. 2018;9(1):1074.
42. Aillon KL, Xie Y, El-Gendy N, Berkland CJ, Forrest ML. Effects of nanomaterial physicochemical properties on in vivo toxicity. *Adv Drug Deliv Rev*. 2009;61(6):457–466.
43. Pedrosa P, Vinhas R, Fernandes A, Baptista PV. Gold nanotheranostics: proof-of-concept or clinical tool? *Nanomaterials*. 2015;5(4):1853–1879.
44. Stern JM, Kibanov Solomonov VV, Sazykina E, Schwartz JA, Gad SC, Goodrich GP. Initial evaluation of the safety of nanoshell-directed photothermal therapy in the treatment of prostate disease. *Int J Toxicol*. 2016;35(1):38–46.
45. Wolinsky JB, Colson YL, Grinstaff MW. Local drug delivery strategies for cancer treatment: gels, nanoparticles, polymeric films, rods, and wafers. *J Control Release*. 2012;159(1):14–26.

Supplementary materials

Table S1 The GFT (°C) corresponding to different contents of F127 and F68 (n=4)

F68	F127		
	20.0%	22.5%	25.0%
0.0%	27.5±0.3	24.8±0.3	21.6±0.4
2.5%	37.7±0.5	31.2±0.4	26.7±0.4
5.0%	44.0±0.8	37.4±0.3	32.6±0.4

Abbreviation: GFT, gel formation temperature.

Table S2 GT of the two different prescriptions (n=4)

	F127 (22.5%) + F68 (2.5%)	F127 (25.0%) + F68 (5.0%)
GT (seconds)	78.3±5.7	116.0±4.2

Abbreviation: GT, gelation time.